AIAA 98-0063

SINGLE-CYCLE AND FATIGUE STRENGTHS OF ADHESIVELY BONDED LAP JOINTS

K. E. Metzinger and T. R. Guess
Senior Members of Technical Staff
Sandia National Laboratories
Albuquerque, New Mexico

Abstract

This study considers a composite-to-steel tubular lap joint in which failure typically occurs when the adhesive debonds from the steel adherend. The same basic joint was subjected to compressive and tensile axial loads (single-cycle) as well as bending loads (fatigue). The purpose of these tests was to determine whether failure is more dependent on the plastic strain or the peel stress that develops in the adhesive. For the same joint, compressive and tensile loads of the same magnitude will produce similar plastic strains but peel stresses of opposite signs in the adhesive. In the axial tests, the tensile strengths were much greater than the compressive strengths - indicating that the peel stress is key to predicting the single-cycle strengths. To determine the key parameter(s) for predicting high-cycle fatigue strengths, a test technique capable of subjecting a specimen to several million cycles per day was developed. In these bending tests, the initial adhesive debonding always occurred on the compressive side. This result is consistent with the single-cycle tests, although not as conclusive due to the limited number of tests. Nevertheless, a fatigue test method has been established and future tests are planned.

Introduction

When adhesively bonded lap joints are utilized as blade attachments in a wind turbine, their performance can significantly impact the operational safety and the economic viability of the turbine. In the interest of improving the durability of these joints, a combined program of testing and analyses is underway. The immediate goal of this effort is to establish which parameter(s) affect the performance of these joints in both single-cycle and fatigue loading, bearing in mind that the key parameter(s) for single-cycle loading may not be the same as those for high-cycle fatigue. The composite-to-steel tubular lap joint considered in this study typically fails when the adhesive debonds from the steel adherend. In order to determine whether this failure is more dependent on the plastic strain or the peel stress that develops in the adhesive near the adhesive/steel adherend interface, the same basic joint was subjected to either compressive or tensile loading.

Axially-loaded specimens were utilized in the single-cycle tests. These specimens were efficiently loaded to failure in both compression and tension with a standard electrohydraulic test frame. However, high-cycle fatigue tests of the joint considered in this study would have been impractical with such a test frame since it can only subject a specimen to approximately a hundred thousand cycles in a single day (allowing for inspections to check for debonding). Thus, a test technique capable of subjecting a specimen to several million cycles per day was developed. After some experimentation, a repeatable fatigue test method utilizing an electromechanical shaker table (for the alternating loads) and bungee cords (for the mean loads) was established. Several specimens were tested in bending until the adhesive was determined - using ultrasonic inspection - to have partially debonded from the steel adherend. During all of the fatigue tests, the alternating loads were less than the mean loads. Thus, one half of each specimen remained in compression and the other half in tension throughout the test. Figure 1 shows a schematic of the compressive (axial) and the bending specimens. The tensile (axial) specimens are the same as the bending specimens with two exceptions. The steel adherends are 4 inches shorter and have internal threads rather than pins at the ends. The adhesive bonds are 2.8 inches long and 0.1 inches thick in all of the specimens.

For the same joint geometry, a compressive load and a tensile load of the same magnitude will produce similar plastic strains in the adhesive. However, the peel stresses that develop in the adhesive where the debonding initiates will be of similar magnitude but opposite sign. (The differences that exist in the magnitudes of the

plastic strains and peel stresses are small and will be addressed with finite element analyses).Thus, the results of the compressive and tensile tests should be comparable or quite different depending on whether the plastic strain or the peel stress, respectively, is the most important parameter influencing failure. In the axial tests, the tensile strengths were much greater than the compressive strengths. Indeed, the tensile specimens (which develop compressive peel stresses in the adhesive) actually failed in the composite - not in the bond itself. This dramatic difference indicates that the adhesive peel stress is key to predicting the single-cycle strength of these joints. In the bending tests, the initial adhesive debonding was always observed on the compressive side - suggesting that the peel stress is more influential than the plastic strain to the fatigue strength of these joints. While this result is consistent with the single-cycle tests, further testing is warranted due to the limited number of samples.

Experiments

1. Specimen Fabrication

Prior to fabrication, the composite (E-glass fabric/ epoxy) and steel adherends were lightly sand blasted, sprayed with isopropyl alcohol and wiped with lint-free cloth. The plastic spacers which are used to fix the location of the bond ends also align the centerlines of the adherends. The adhesive (Hysol EA-9394) was injected into the joints and allowed to cure at room temperature for one week before the plastic spacers were removed. For the double-jointed specimens, the same process is repeated for the second joint. (The tensile and bending tests use double-jointed specimens due to fixture constraints.) For the fatigue (bending) specimens, the plastic spacer which is trapped inside the composite tube (subsequent to curing of the second joint) was removed prior to testing.

2. Single-Cycle (Axial) Tests

The compressive and tensile specimens were tested in an electrohydraulic test frame. Figure 2 shows a compressive specimen between two platens. The tensile specimens were attached to the test frame with eyebolts which were screwed into the threaded ends of the steel adherends. The composite adherend of each specimen was instrumented with three strain gages - equally spaced along the circumference - to verify that it was uniformly loaded.

Figure 3 shows the failure loads recorded for the axial tests. Note that the compressive specimens failed at much lower levels than the tensile specimens. For the compressive specimens, failure occurred abruptly - at an average load of approximately 35000 lb - when the adhesive completely debonded from the steel adherend. However, the levels shown for the tensile specimens represent the applied load when the composite adherend failed. The adhesive didn't actually debond from the steel. Thus, the difference in single-cycle strengths for compressive and tensile loading is at least as great as the data in Figure 3 suggests since the tensile joints didn't actually fail. One final point should be made. Each tensile specimen has two joints. Therefore, four (not two) joints were loaded in tension to over 70000 lb without debonding.

3. Fatigue (Bending) Tests

Figure 4 shows the setup used for the fatigue testing. The pins on both ends of the specimen fit inside lubricated composite bushings which were inserted into steel cylinders. In turn, these cylinders were clamped into the aluminum fixture which was attached to the shaker table. Copper tape was applied to the composite where the kevlar strap loops around the specimen. This step was taken to reduce the frictional heating that occurred at this location. Fans were also utilized to minimize any temperature increases of the specimen during testing. The low spring stiffness (~100 lb/in) of the bungee cords allowed a nearly constant lateral load to be applied to the center of a specimen even as it vibrated due to the input from the shaker table. Strain gages were attached to the top and bottom of each composite adherend at an axial location near the middle of one of the bonds. Accelerometers were typically mounted on the side of the specimens.

Figure 5 shows the results of the fatigue tests. Each test was terminated as soon as the adhesive was determined - using a pulse/echo ultrasonic inspection technique - to have partially debonded from the steel adherend in either joint. At this point, the debonded region extends over a very small portion (0.5 in^2 or less) of the originally bonded region. Note that the alternating load is given in terms of the base excitation since it is closely controlled. Although the response of the

specimens is roughly proportional to the input, it appears to fall off a little at the higher input levels. The mean and alternating components of the strains measured on the bottom and top surfaces of the composite tubes are listed in Tables 1 and 2. All the specimens were subjected to a mean load of 750 lb as well as an alternating load at 200 Hz.

Several points should be made regarding this data. Note that the alternating strains were always smaller than the mean strains. Thus, the top half of each specimen remained in tension while the bottom half remained in compression. In the six specimens in which the adhesive debonded from the steel adherend, the debonding always occurred on the compressive side. This result is consistent with the results of the single-cycle tests, but not as conclusive since the magnitudes of the mean composite surface strains (and presumably the adhesive peel stresses) are higher on the compressive side. However, the alternating composite strains are lower on the compressive side. The difference in the mean strains is probably due in part to the way in which the specimens were loaded with the kevlar strap and will subsequently be addressed with finite element analyses. The cause of the differences in the alternating strains hasn't been determined. A further complication is that even for a given specimen and location (bottom or top side), the tensile and compressive peaks of the alternating loads typically differ, at least for the higher inputs. (Although the input was sinusoidal and the response of the specimens consisted primarily of the first bending mode, the second bending mode was also excited, particularly at the higher levels.)

Regardless of the exact magnitudes of the composite strains, the adhesive in the top and bottom halves of a bending specimen experienced peel stresses that differed somewhat in magnitude as well as sign. Currently, its unclear as to whether the differences in magnitude are significant. Minor modifications to the testing procedure may be able to minimize any differences due to the test setup or frequency. However, it may not be practical to reduce any differences which are due to the material response differing with the loading (compressive versus tensile). Although minor modifications may be implemented, a high-cycle fatigue test methodology has been developed and is available for the future testing which is planned.

Analyses

1. Finite Element Models

Figure 6 shows the axisymmetric finite element mesh used for the compressive specimen. The adhesive layer has four elements through its thickness. The finite element mesh of the tensile specimen employs a symmetry plane and is similar to the mesh shown in Figure 6 except that the lengths of the adherends are different. Both meshes are comprised of eight-node biquadratic axisymmetric solid elements (CAX8). Figure 7 shows the finite element model used for the bending specimen. Note that two symmetry planes are utilized in this three-dimensional mesh, which is comprised of twenty-node quadratic hex elements (C3D20). Although the bending mesh is coarser (one element through the thickness for the adhesive and the adherends) than the axial meshes, it is adequate for assessing the effect of the wrap angle of the kevlar strap. All of the analyses - which incorporate nonlinear geometric effects and allow for plastic deformations in the adhesive - were performed with ABAQUS[1]. The isotropic material properties used for the adhesive[2] and the steel are listed in Table 3. Generic values were used for the steel. The adhesive properties correspond to a high strength, room-temperature curing paste adhesive. The orthotropic material properties[3] listed in Table 4 represent a plain weave E-glass fabric/epoxy composite. The subscripts *r*, *a*, and *t* in Table 4 refer to the radial, axial, and tangential directions, respectively.

2. Axial Specimens

Figures 8 and 9 show the plastic strains and peel stresses that develop in the adhesive at the adhesive/steel adherend interface, respectively, for an axial load of 35000 lb. (Although the calculated values are dependent upon the corresponding finite element mesh, the same discretization was used to model the compressive and tensile specimens.) The end of the bond where failure initiates (the right end in Figure 6) corresponds to an axial location of 2.8 inches. Note that the adhesive yielding is very similar for the compressive and tensile specimens. Although the peel stresses have opposite sign, their magnitudes are also quite similar. The small differences (6 and 10% for the peak values of the plastic strain and the peel stress, respectively) that exist in the magnitudes arise from nonlinear geometric effects

and may not be significant. Regardless, the plastic strain in the adhesive of a tensile specimen is at least as great as that in a compressive specimen. Thus, if the adhesive yielding is the key to the single-cycle joint strength, the tensile specimens shouldn't be significantly stronger than the compressive specimens. Given the experimental results in which the tensile strengths were at least twice the compressive strengths, it is clear that the peel stress is a key parameter affecting the single-cycle strengths of these joints. The tensile peel stresses that develop in the adhesive cause it to debond from the steel adherend. Although the plastic strain in the adhesive isn't as important as the peel stress, it may influence the single-cycle strengths of these joints to a lesser extent.

3. Bending Specimens

As mentioned earlier, the bending finite element model was constructed to determine if the wrap angle of the kevlar strap could have caused at least some of the differences in the strain data for the bottom and top halves of the specimens. Figure 10 shows a sketch of a strap wrapped around a specimen. Unfortunately, the fatigue test setup was disassembled before the effect of the wrap angle was considered and no measurements of it were made. Accordingly, several possible wrap angles were considered and the results of these analyses are listed in Table 5. The tabulated composite strain values predicted by the analyses demonstrate that increasing the wrap angle beyond 90 degrees will lead to compressive strains with larger magnitudes than the tensile strains, as was observed experimentally (see Table 1). Although no adhesive yielding was predicted for a 750 lb load with this relatively coarse mesh, the differences in the peak von Mises stresses in the adhesive are similar to those seen in the composite strains. Thus, a wrap angle of 90 degrees is desirable for balancing the magnitudes of the stresses in the adhesive on the bottom and top sides of a specimen. Although it is not presently known how much of the measured strain differences were due to the wrap angle, it appears that any such differences can be eliminated in future tests.

Summary

The durability of adhesively bonded lap joints directly affects the viability of wind turbines that utilize these joints as blade attachments. The purpose of this study was to establish which parameter(s) affect the performance of these joints. Both single-cycle and fatigue were considered. Single-cycle axial tests which subjected the same basic joint geometry to either compressive and tensile loading were used to establish that the peel stress in the adhesive is the key parameter affecting the single-cycle strength of the tubular lap joints considered in this study. In addition, a novel fatigue test method was developed. The limited fatigue data suggests that the adhesive peel stress is also critical to the fatigue strengths of these joints. Although more fatigue testing is warranted, a practical technique that is capable of subjecting a bending specimen to several million cycles in a single day has been developed and will be available for future tests.

Acknowledgments

M. E. Stavig performed the single-cycle tests of the joints. D. W. Kelton conducted the fatigue tests and made improvements to the test setup. T. G. Rice was responsible for the prototype testing and fixtures. This work was performed at Sandia National Laboratories, which is operated for the U. S. Department of Energy under Contract No. DE-AC04-94AL85000.

References

1. ABAQUS/Standard, Version 5.6.
2. T. R. Guess, E. D. Reedy, Jr., and M. E. Stavig, "Mechanical Properties of Hysol EA-9394 Structural Adhesive," SAND95-0229, Sandia National Laboratories, Albuquerque, New Mexico, February 1995.
3. T. R. Guess, E. D. Reedy, Jr., and A. M. Slavin, "Testing Composite-to-Metal Tubular Lap Joints," *Journal of Composites Technology & Research*, Vol. 17, No. 2, April 1995.

Table 1: Mean Composite Strains - Tests

Specimen	Bottom Side Strain (με)	Top Side Strain (με)	|Ratio|
A	-245	+229	1.07
B	-248	+221	1.12
C	-228	+221	1.03
D	-253	+220	1.15
E	-239	+215	1.11
F	-256	+220	1.16
G	-252	+210	1.20
H	-240	+221	1.09
Average	-245	+220	1.12

Table 2: Alternating Composite Strains - Tests

Specimen	Shaker (±g)	Bottom Side Strain (με)	Top Side Strain (με)
A	30	+113/-115	+124/-123
B	35	+132/-132	+142/-140
C	35	+126/-130	+149/-144
D	40	+159/-145	+152/-161
E	40	+151/-145	+155/-158
F	45	+172/-159	+167/-175
G	45	+179/-166	+170/-178
H	45	+164/-155	+174/-175

Table 3: Isotropic Material Properties

Material	Elastic Modulus (psi)	Poissons Ratio
Adhesive	6.0×10^5	0.37
Steel	3.0×10^7	0.30
Material	**Yield Strength (psi)**	**Hardening Modulus (psi)**
Adhesive	4.0×10^3	3.0×10^5
Steel	-	-

Table 4: Composite Orthotropic Material Properties

E_r (psi)	E_a (psi)	E_t (psi)
1.45×10^6	3.26×10^6	4.06×10^6
υ_{ra}	υ_{rt}	υ_{at}
0.10	0.10	0.17
G_{ra} (psi)	G_{rt} (psi)	G_{at} (psi)
7.25×10^5	7.25×10^5	7.25×10^5

Table 5: Mean Composite Strains - Analyses

Wrap Angle (degrees)	Bottom Side Strain (με)	Top Side Strain (με)	|Ratio|
90	-224	+225	1.00
99	-228	+219	1.04
108	-233	+214	1.09
117	-237	+209	1.13

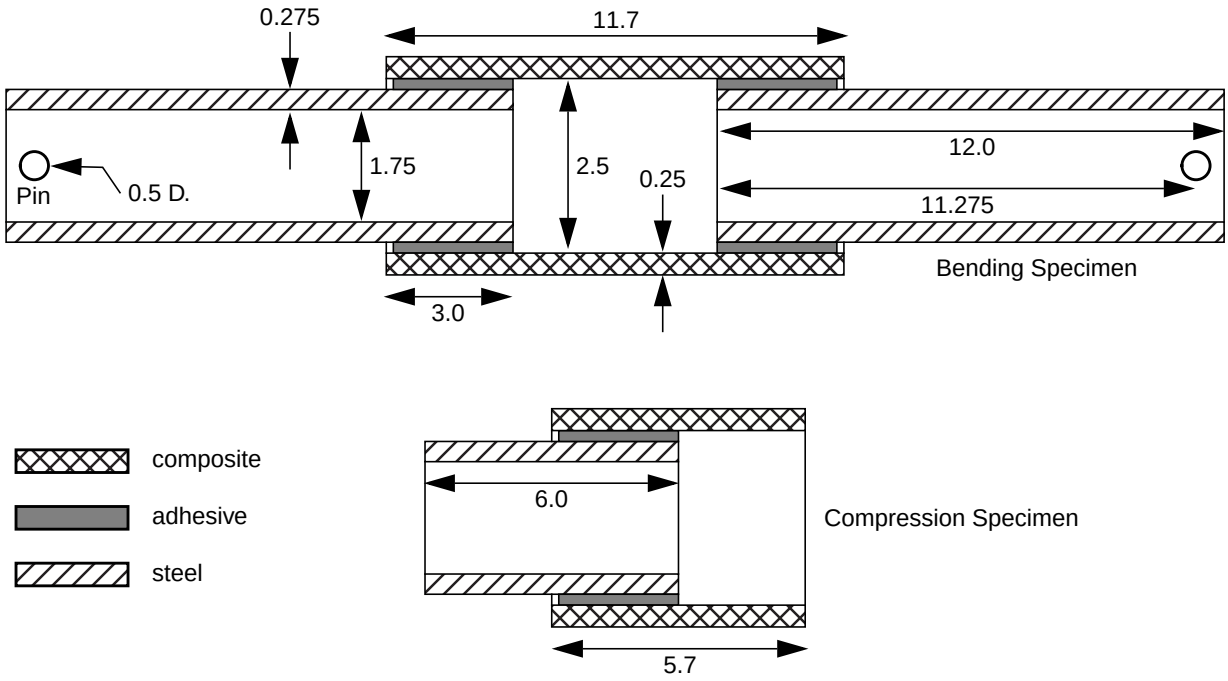

Figure 1. Schematic of Joint Geometries (Cut-away View, Dimensions in Inches)

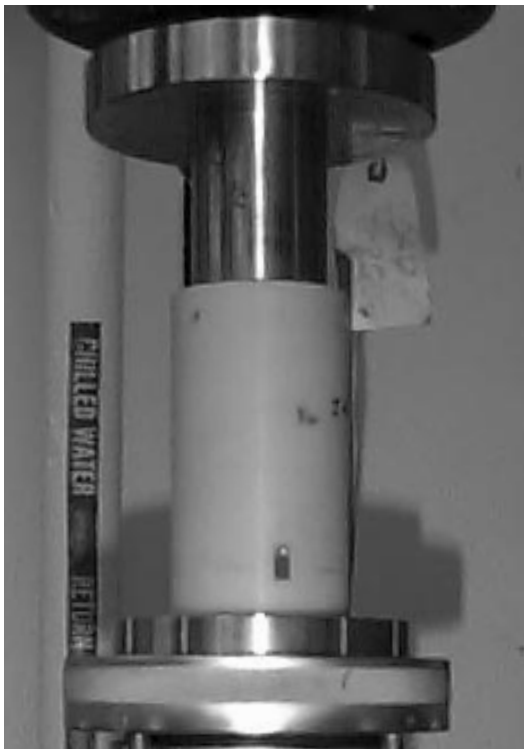

Figure 2. Single-Cycle (Compressive) Test Setup

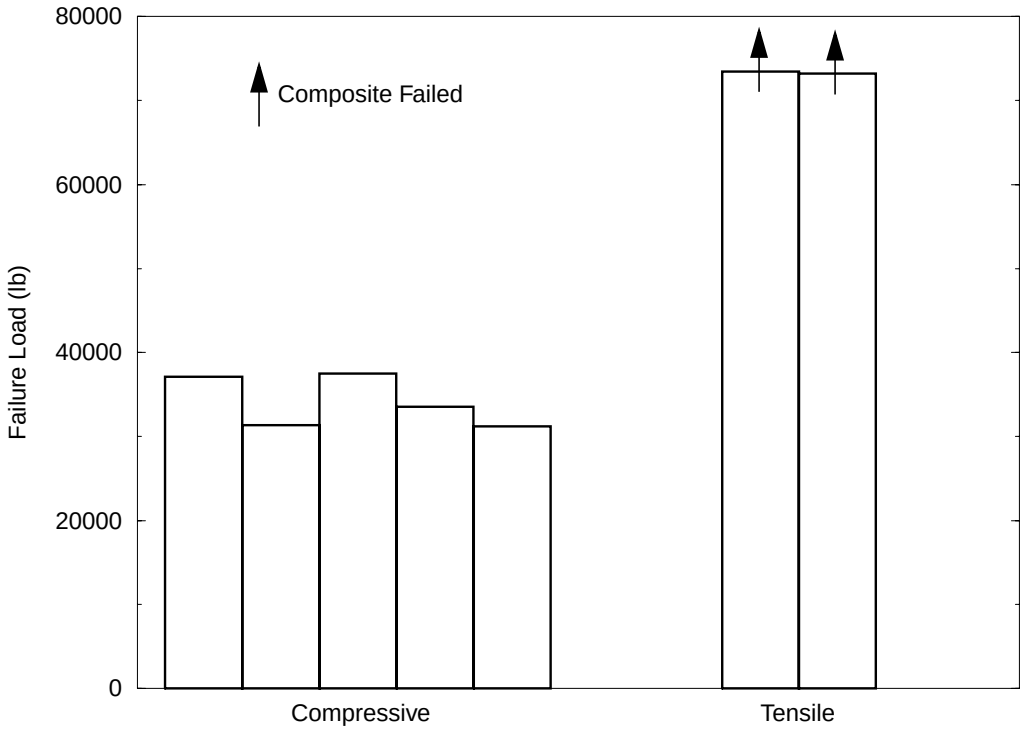

Figure 3. Single-Cycle Failure Loads

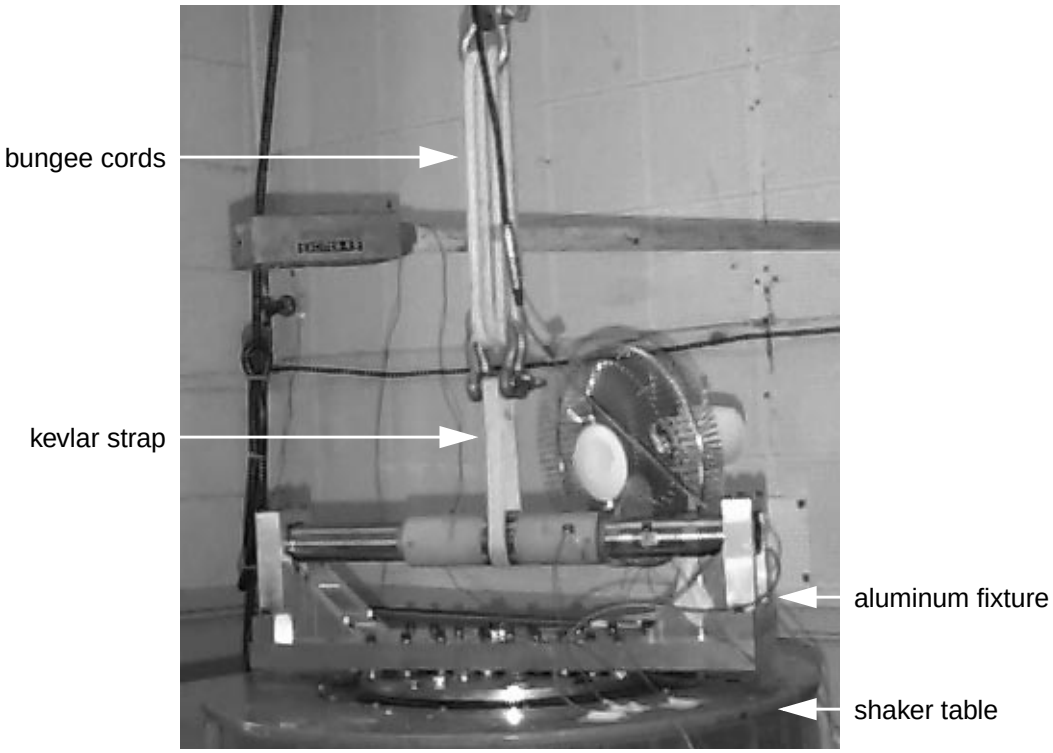

Figure 4. Fatigue Test Setup

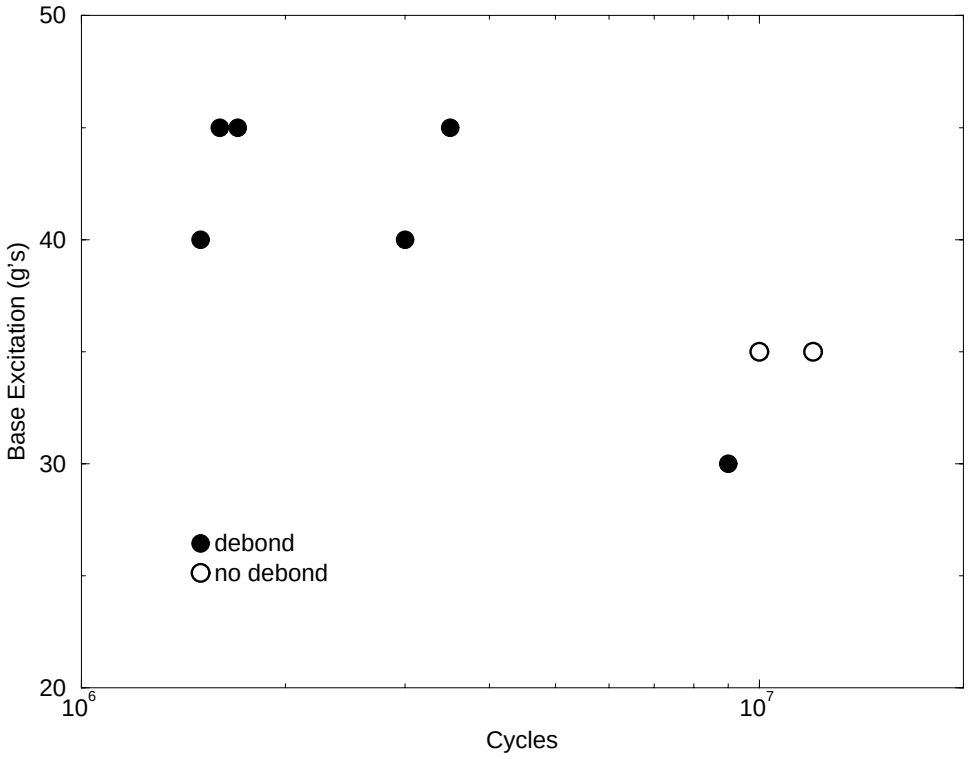

Figure 5. Fatigue Test Results

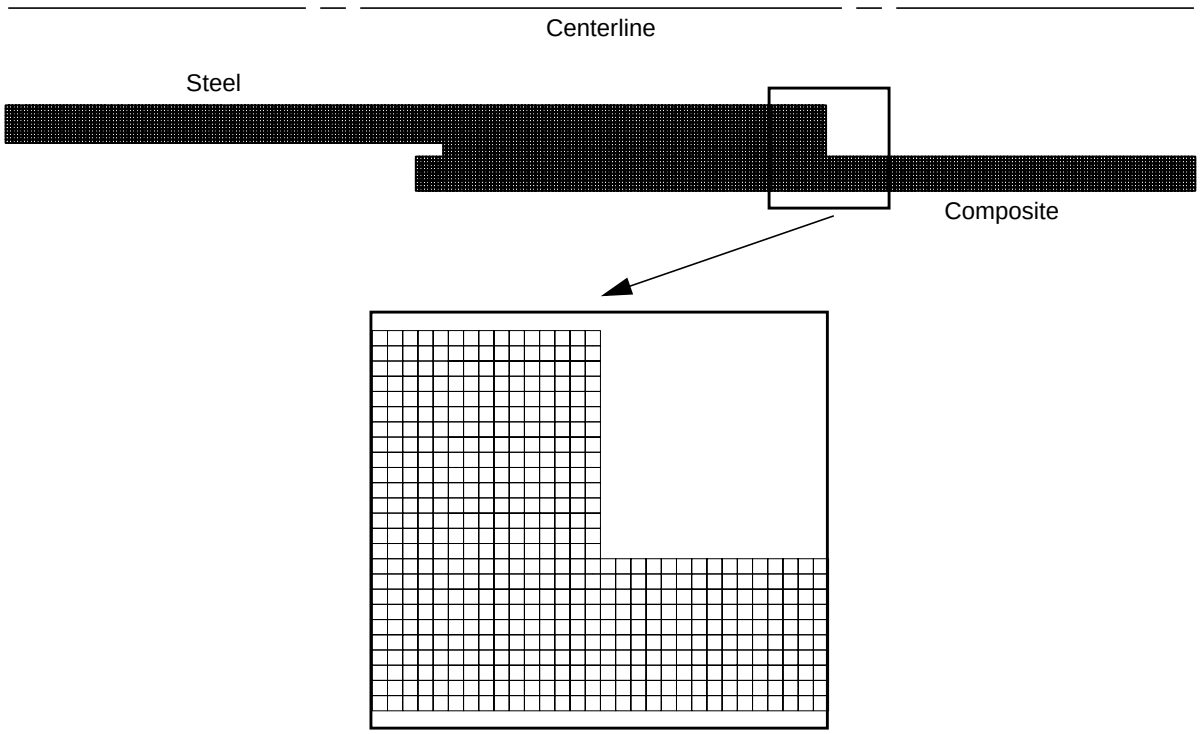

Figure 6. Axisymmetric Finite Element Mesh (Compressive Specimen)

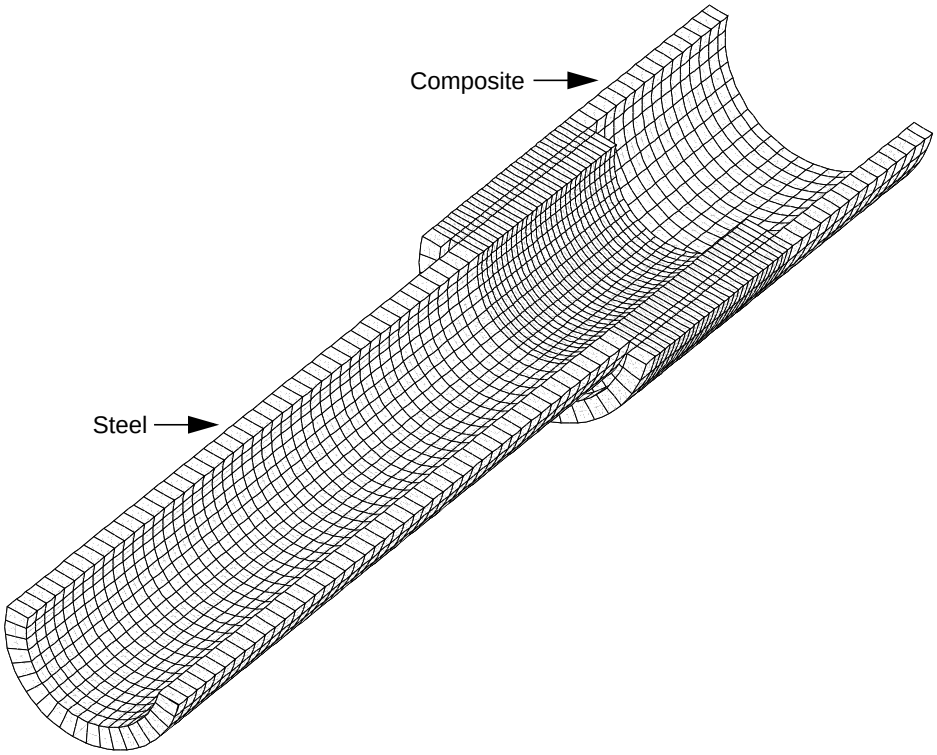

Figure 7. Three-Dimensional Finite Element Mesh (Bending Specimen)

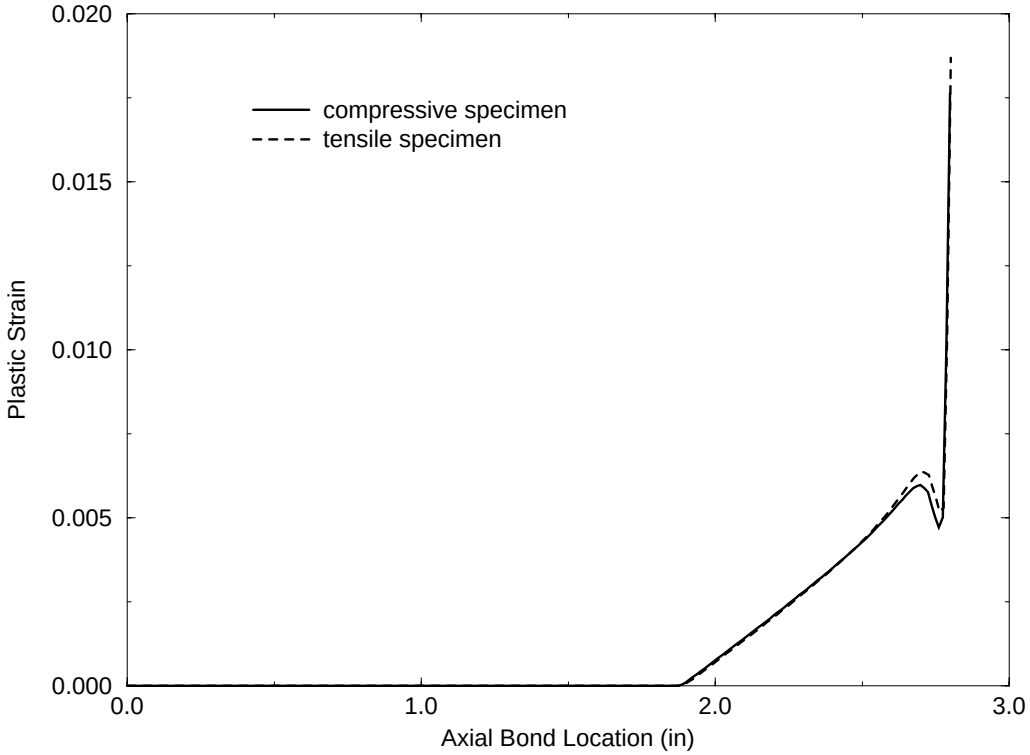

Figure 8. Adhesive Plastic Strains

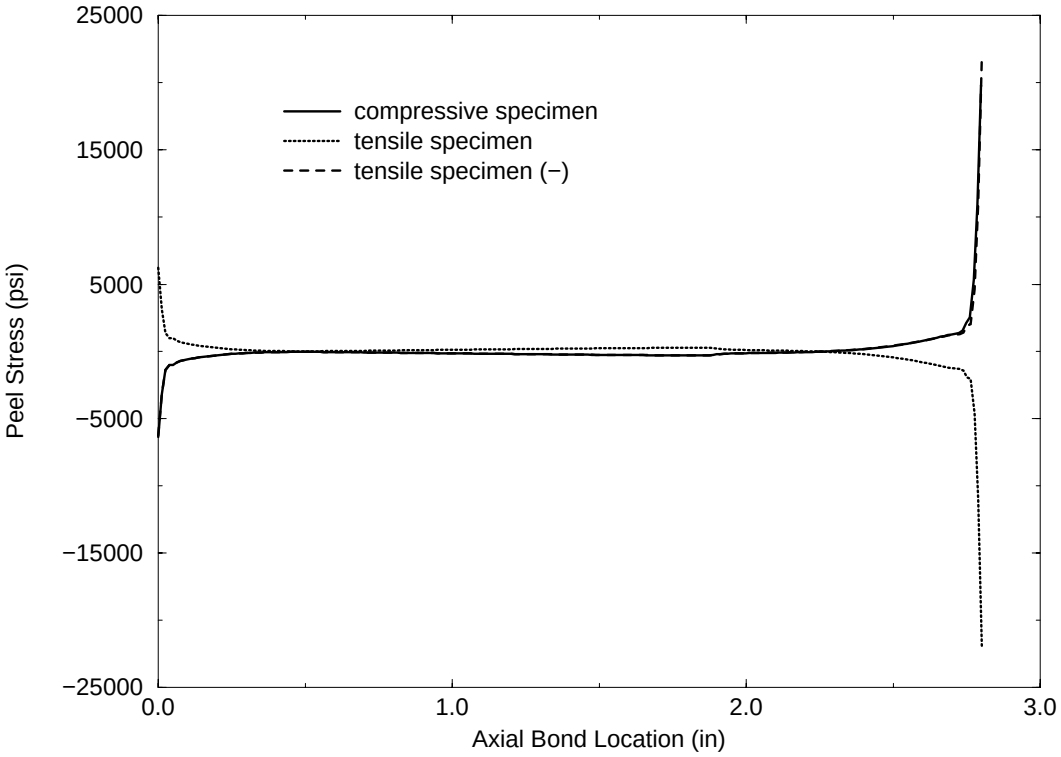

Figure 9. Adhesive Peel Stresses

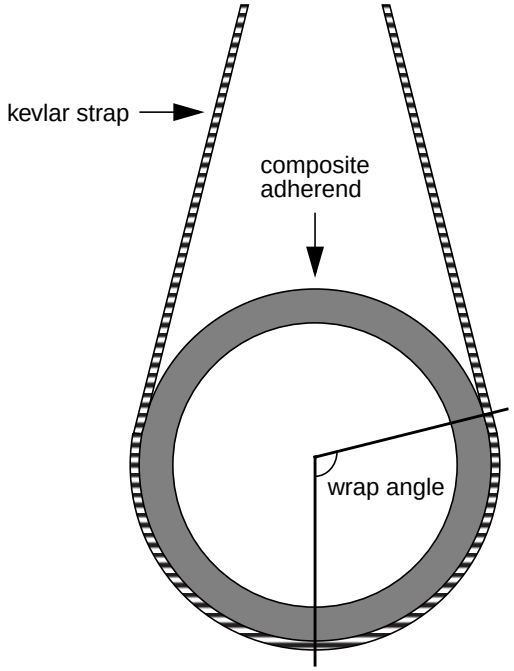

Figure 10. Strap Wrapped Around Specimen